

1 International Journal of Modern Physics E
 2 © World Scientific Publishing Company

4 **Study of Electromagnetic Effect by Charged-dependent Directed Flow**
 5 **in Isobar Collisions at $\sqrt{s_{NN}} = 200$ GeV using STAR at RHIC**

6 Dhananjaya Thakur (for the STAR collaboration)
 7 *Institute of Modern Physics, Chinese Academy of Sciences, Lanzhou, Gansu,*
 8 *730000, China*
 9 *dhananjaya.thakur@impcas.ac.cn*

10 Received Day Month Year
 11 Revised Day Month Year

12 In non-central heavy-ion collisions, it is predicted that an initial strong but transient
 13 magnetic field ($\sim 10^{18}$ Gauss) can be generated. The charge-dependent directed flow
 14 (v_1) can serve as the probe to detect this initial magnetic field. In addition, v_1 of several
 15 identified hadron species with different constituent quarks will help to disentangle the
 16 role of produced and transported quarks. In this proceedings, we present the measure-
 17 ments of v_1 for π^\pm , K^\pm , $p(\bar{p})$ in Ru+Ru and Zr+Zr collisions at $\sqrt{s_{NN}} = 200$ GeV as
 18 a function of transverse momentum, rapidity, and centrality. The difference of v_1 slope
 19 ($\Delta dv_1/dy$) between protons and anti-protons is observed and is studied as a function of
 20 centrality. While the contribution from transported quarks can give positive $\Delta dv_1/dy$,
 21 the electromagnetic field is predicted to give negative $\Delta dv_1/dy$. The significant negative
 22 $\Delta dv_1/dy$ of protons in peripheral collisions is consistent with the prediction from initial
 23 strong magnetic field in heavy-ion collisions.

24 *Keywords:* heavy-ion collisions; directed flow; electromagnetic effect; transported-quark.

25 *PACS numbers:*

26 **1. Introduction**

27 A collision of two ultra-relativistic nuclei forms a strongly interacting matter called
 28 the Quark-Gluon Plasma (QGP).⁴ Anisotropic flow is quantified by Fourier coef-
 29 ficients of particle's distribution in azimuthal angle measured with respect to the
 30 reaction plane. The first coefficient of Fourier expansion is termed as directed flow
 31 (v_1),⁵

$$v_1 = \langle \cos(\phi - \Psi_R) \rangle, \quad (1)$$

32 where ϕ denotes the azimuthal angle of an outgoing particle and Ψ_R is the orien-
 33 tation of the reaction plane defined by the beam axis and the impact parameter
 34 vector. The rapidity-odd component of directed flow $v_1(y)$ has been argued to be
 35 sensitive to initial strong electromagnetic (EM) fields.³

36 In the early stages of the collisions, an ultra strong magnetic field is expected
 37 to be created ($eB \sim m_\pi^2$ at top Relativistic Heavy Ion Collider (RHIC) energy).⁶

38 This magnetic field is generated by the incoming spectator protons in the collision,
 39 and may be captured if the medium produced has finite electric conductivity. As
 40 the spectator protons recede from the collision zone the produced magnetic field
 41 decays with time. This time-varying magnetic field induces an electric field due to
 42 the Faraday effect. The Lorentz force results in an electric current perpendicular to
 43 expansion velocity of medium and magnetic field, akin to the classical Hall effect.
 44 The interplay of competing Faraday and Hall effects can influence the v_1 . In other
 45 words, EM fields are expected to drive positively-charged and negatively-charged
 46 particles in opposite ways, leading to a splitting of $v_1(y)$.³

47 UrQMD calculations⁸ at RHIC energies have shown that the transported protons
 48 and the spectator nucleons have the same sign of v_1 and hence they have a
 49 positive v_1 slope ($dv_1/dy > 0$) at the mid-rapidity. On the other hand, produced
 50 protons and anti-protons can have negative v_1 ($dv_1/dy < 0$) slope due to contribu-
 51 tion other than transported quarks, e.g. the tilted source.⁷ This results in a positive
 52 splitting between protons and anti-protons [$\Delta dv_1/dy = dv_1/dy(p) - dv_1/dy(\bar{p}) > 0$].
 53 Therefore, transport will affect the splitting between any particle and anti-particle
 54 pairs having transported quark content, e.g splitting between $\pi^+(u\bar{d})$ and $\pi^-(d\bar{u})$,
 55 and also between $K^+(u\bar{s})$ and $K^-(\bar{u}s)$. Finally, the interplay between EM field and
 56 transported quark effect determines the sign and magnitude of splitting between
 57 particle and anti-particle pairs.

58 2. Method and Analysis

59 This analysis uses Ru+Ru and Zr+Zr collisions at $\sqrt{s_{NN}} = 200$ GeV, collected by
 60 Solenoidal Tracker at RHIC (STAR) during 2018. Details about the event cuts and
 61 track selections can be found in Ref.⁹ In this analysis, the first order event plane
 62 angle is determined using Zero Degree Calorimeter (ZDC).¹⁰ The description of
 63 measuring v_1 using the ZDC event plane can be found in Ref.⁹ The Time Projection
 64 Chamber (TPC)¹¹ was used for charged-particle tracking within pseudorapidity
 65 $|\eta| < 1$, with full 2π azimuthal coverage. After the vertex selection, we analysed
 66 about 1.7 billion Ru+Ru events and 1.8 billion Zr+Zr events. Centrality is defined
 67 from the number of charged particles detected by the TPC within $|\eta| < 0.5$. The
 68 directed flow analyses were carried out on tracks that have transverse momenta,
 69 $p_T > 0.2$ GeV/c for π^\pm and K^\pm , and $p_T > 0.4$ GeV/c for $p(\bar{p})$. The tracks should
 70 pass a requirement to be within 3 cm of distance of closest approach (DCA) to
 71 the primary vertex (V_z), and have at least 15 space points (N_{hits}) in the main
 72 TPC acceptance. π^\pm , K^\pm , p and \bar{p} are identified based on the truncated mean
 73 value of the track energy loss ($\langle dE/dx \rangle$) in the TPC and we select $|n\sigma| < 2$ ($n\sigma =$
 74 $\frac{1}{\sigma_R} \ln(\langle dE/dx \rangle / \langle dE/dx \rangle_{[\pi/K/p]})$, σ_R is the $\langle dE/dx \rangle$ resolution). To ensure the purity
 75 of identified particles, we select particles with momentum smaller than 2 GeV/c for
 76 protons, and 1.6 GeV/c for pions and kaons. The time-of-flight detector (TOF)¹²
 77 was used to improve the particle identification and we select particles within mass-
 78 square (m^2) range, $-0.01 < m^2 < 0.1$ ((GeV/c²)²) for pions, $0.2 < m^2 < 0.35$

79 $((\text{GeV}/c^2)^2)$ for kaons and $0.8 < m^2 < 1.0$ $((\text{GeV}/c^2)^2)$ for protons.

80 The systematic uncertainties of the v_1 measurements are calculated by vary-
 81 ing DCA, V_z , N_{hits} , $n\sigma$ etc. within a reasonable maximum range. The absolute
 82 difference ($|\Delta_i|$) between default cut with the cut variation is taken as systematic
 83 uncertainty. In addition, the absolute difference between the $v_1(y)$ slopes between
 84 forward and backward rapidities is also considered as a source of systematic uncer-
 85 tainty. The final systematic error is the quadrature sum of the systematic errors
 86 from all the sources, which are calculated as $|\Delta_i|/\sqrt{12}$ assuming uniform probability
 87 distribution.

88 3. Results

89 Figure 1 presents $v_1(y)$ for protons and anti-protons in Au+Au collisions at
 90 $\sqrt{s_{NN}} = 27$ and 200 GeV and isobar collisions at $\sqrt{s_{NN}} = 200$ GeV in the cen-
 91 trality range of 50–80%. Linear fits within $-0.8 < y < 0.8$ (solid lines) that passing
 92 through $(0, 0)$ is used to extract the slope ($\Delta dv_1/dy$). We observe a significant
 93 negative slope of proton and antiproton difference in the peripheral collisions which
 94 is inline with the prediction of dominance of the Faraday/Coulomb effect over the
 95 Hall and transported-quark effects, as transported quarks only provide positive con-
 96 tributions to the proton $\Delta dv_1/dy$.⁸ The extracted $\Delta dv_1/dy$ values for each particle
 97 species using the same linear-function fit are plotted as a function of centrality and
 98 is presented in Fig. 2 for π^\pm , K^\pm , p and \bar{p} in Au+Au at $\sqrt{s_{NN}} = 27$ and 200 GeV
 99 and isobar collisions at $\sqrt{s_{NN}} = 200$ GeV.

100 It is clear from Fig. 2 that $\Delta dv_1/dy$ for protons shows decreasing trend, i.e
 101 positive to negative when going from central to peripheral collisions. The electro-
 102 magnetic effect is weak in central collisions due to the lack of spectator protons.
 103 Therefore, the transported-quark effect can contribute to the positive v_1 splitting.
 104 Towards the peripheral collisions the electromagnetic effect can be dominant and
 105 we see a sign change of $\Delta dv_1/dy$. The solid curve represented in the figure shows
 106 the quantitative calculation of electromagnetic-field contributions to the proton
 107 $\Delta dv_1/dy$ in Au+Au collisions at $\sqrt{s_{NN}} = 200$ GeV.² Similar decreasing trend of
 108 $\Delta dv_1/dy$ is also observed for K^+ and K^- , but less significant compared to protons.
 109 This could be due to the fact that kaons have lower mean transverse momentum
 110 ($\langle p_T \rangle$) than protons and hence weaker electromagnetic field effects.²

111 The v_1 splitting between π^+ and π^- is consistent with zero within uncertainty at
 112 $\sqrt{s_{NN}} = 200$ GeV. The transported quarks should give negative $\Delta dv_1/dy$ between
 113 π^+ and π^- . Also, the electromagnetic effect gives negative $\Delta dv_1/dy$. Since π^+ and
 114 π^- numbers are almost symmetric at the top RHIC energy, the transported-quark
 115 effect is negligible. The electromagnetic effect can be diluted from neutral resonance
 116 decay. At $\sqrt{s_{NN}} = 27$ GeV, we can see a small negative $\Delta dv_1/dy$ at peripheral
 117 collisions which can have both transported-quark and electromagnetic effect.

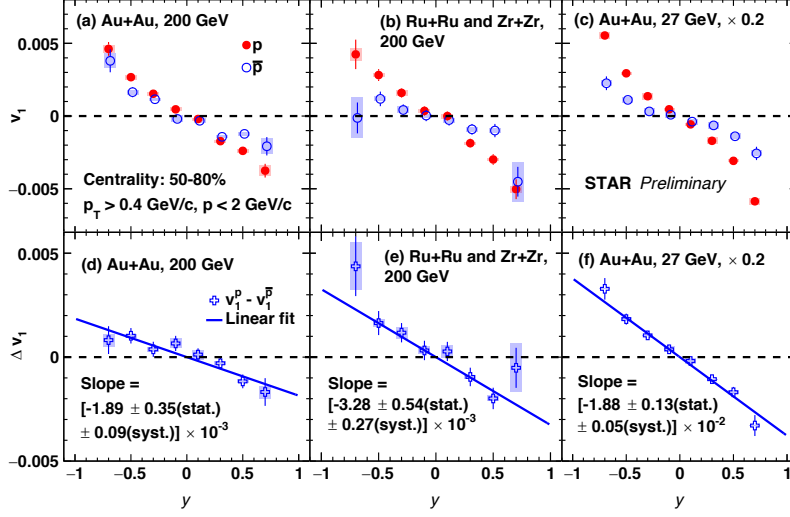


Fig. 1. Directed flow of protons and anti-protons and their difference ($v_1^p - v_1^{\bar{p}}$) as a function of rapidity for Au+Au collisions at $\sqrt{s_{NN}} = 27$ and 200 GeV, and Ru+Ru and Zr+Zr collisions at $\sqrt{s_{NN}} = 200$ GeV for 50-80 % centrality.¹ The systematic uncertainties are indicated with shaded bands and the slopes are obtained with linear fits (solid lines).

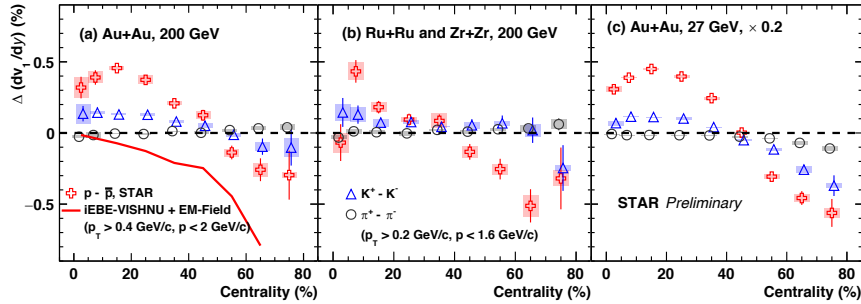


Fig. 2. Slope difference ($\Delta(dv_1/dy)$) between positively and negatively charged pions, kaons and protons as a function of centrality for Au+Au collisions at $\sqrt{s_{NN}} = 27$ and 200 GeV and isobar collisions at $\sqrt{s_{NN}} = 200$.¹ The systematic uncertainties are represented by shaded bands. The solid line is the electromagnetic field prediction for v_1 splitting between protons and anti-protons in Au+Au collisions at $\sqrt{s_{NN}} = 200$ GeV.²

118 4. Summary and Outlook

119 The study of charged-dependent v_1 can provide information about transported
 120 quark and electromagnetic (Hall, Faraday, and Coulomb etc.) effects in heavy-ion
 121 collisions. We have presented the v_1 measurements of π^\pm , K^\pm , p and \bar{p} for Au+Au
 122 collisions at $\sqrt{s_{NN}} = 27$ and 200 GeV, and Ru+Ru and Zr+Zr collisions at $\sqrt{s_{NN}} =$

123 200 GeV. The splitting between protons and anti-protons changes sign from posi-
 124 tive value in central collisions to negative value in peripheral collisions. The positive
 125 value of $\Delta dv_1/dy$ in central collisions could be accommodated by transported quark
 126 contribution where as significant negative $\Delta dv_1/dy$ in peripheral collisions is consis-
 127 tent with expectation from dominance of Faraday/Coulomb effects over Hall effect.

128 References

- 129 1. Observation of the electromagnetic field effect via charge-dependent directed flow in
 130 Au+Au, Ru+Ru, and Zr+Zr collisions at $\sqrt{s_{NN}} = 200$ GeV (In preparation by STAR
 131 collaboration).
- 132 2. U. Gürsoy, D. Kharzeev, E. Marcus, K. Rajagopal and C. Shen, "Charge-dependent
 133 Flow Induced by Magnetic and Electric Fields in Heavy Ion Collisions," Phys. Rev. C
 134 **98** (2018), 055201
- 135 3. U. Gürsoy, D. Kharzeev and K. Rajagopal, "Magnetohydrodynamics, charged currents
 136 and directed flow in heavy ion collisions," Phys. Rev. C **89** (2014), 054905
- 137 4. E. Shuryak, "Strongly coupled quark-gluon plasma in heavy ion collisions," Rev. Mod.
 138 Phys. **89** (2017), 035001
- 139 5. L. Adamczyk *et al.* [STAR], "Directed Flow of Identified Particles in Au + Au Collisions
 140 at $\sqrt{s_{NN}} = 200$ GeV at RHIC," Phys. Rev. Lett. **108** (2012), 202301
- 141 6. V. Voronyuk, V. D. Toneev, W. Cassing, E. L. Bratkovskaya, V. P. Konchakovski and
 142 S. A. Voloshin, "(Electro-)Magnetic field evolution in relativistic heavy-ion collisions,"
 143 Phys. Rev. C **83** (2011), 054911
- 144 7. P. Bozek and I. Wyskiel, "Directed flow in ultrarelativistic heavy-ion collisions," Phys.
 145 Rev. C **81** (2010), 054902
- 146 8. Y. Guo, F. Liu and A. Tang, "Directed flow of transported and non-transported protons
 147 in Au+Au collisions from UrQMD model," Phys. Rev. C **86** (2012), 044901
- 148 9. J. Adams *et al.* [STAR], "Azimuthal anisotropy at RHIC: The First and fourth har-
 149 monics," Phys. Rev. Lett. **92** (2004), 062301
- 150 10. C. Adler, A. Denisov, E. Garcia, M. J. Murray, H. Strobele and S. N. White, "The
 151 RHIC zero degree calorimeter," Nucl. Instrum. Meth. A **470** (2001), 488-499
- 152 11. M. Anderson, J. Berkovitz, W. Betts, R. Bossingham, F. Bieser, R. Brown, M. Burks,
 153 M. Calderon de la Barca Sanchez, D. A. Cebra and M. G. Cherney, *et al.* "The Star
 154 time projection chamber: A Unique tool for studying high multiplicity events at RHIC,"
 155 Nucl. Instrum. Meth. A **499** (2003), 659-678
- 156 12. W. J. Llope, F. Geurts, J. W. Mitchell, Z. Liu, N. Adams, G. Eppley, D. Keane, J. Li,
 157 F. Liu and L. Liu, *et al.* Nucl. Instrum. Meth. A **522** (2004), 252-273